# 2007 Fall Technical Meeting Eastern States Section of the Combustion Institute University of Virginia October 21-24, 2007

# Supersonic combustion research at NASA

J. Philip Drummond<sup>1</sup>, Paul M. Danehy<sup>2</sup>, Daniel Bivolaru<sup>3</sup>, Richard L. Gaffney<sup>4</sup>, Sarah A. Tedder<sup>5</sup> and Andrew D. Cutler<sup>6</sup>

<sup>1</sup>Hypersonic Airbreathing Propulsion Branch
<sup>2</sup>Advanced Sensing and Optical Measurements Branch
<sup>3</sup>NASA Post-Doctoral Fellow
<sup>4</sup>Hypersonic Air Breathing Propulsion Branch
<sup>5</sup>NASA Graduate Coop and Research Assistant, College of William and Mary,
NASA Langley Research Center, Hampton, Virginia 23681, USA
<sup>6</sup>Department of Mechanical and Aerospace Engineering, The George Washington University,
Newport News, Virginia 23606, USA

This paper discusses the progress of work to model high-speed supersonic reacting flow. The purpose of the work is to improve the state of the art of CFD capabilities for predicting the flow in high-speed propulsion systems, particularly combustor flowpaths. The program has several components including the development of advanced algorithms and models for simulating engine flowpaths as well as a fundamental experimental and diagnostic development effort to support the formulation and validation of the mathematical models. The paper will provide details of current work on experiments that will provide data for the modeling efforts along with the associated nonintrusive diagnostics used to collect the data from the experimental flowfield. Simulation of a recent experiment to partially validate the accuracy of a combustion code is also described.

#### 1 Introduction

The design and development of a propulsion system is accomplished with several levels of analytic tools, ground-based testing and finally flight. This paper will discuss the progress of work to improve the state of the art of CFD capabilities for predicting high-speed reacting flow in engines. The research has several components including the development of advanced algorithms and models for simulating engine flowpaths as well as a fundamental experimental and diagnostic development effort to support the formulation and validation of the mathematical models. The paper will provide details of current work on experiments and the associated non-intrusive diagnostics that will provide data for the modeling efforts. This effort will lead to the development of phenomenological models for Reynolds averaged Navier-Stokes codes, subgrid scale models for large-eddy simulation techniques, and reduced-kinetics models that can then be applied to the design of high-speed propulsion systems.

## 2 Axisymmetric Coaxial Free Jet Experiments and Related Design Computations

Computational fluid dynamics (CFD) methods that employ the Reynolds-averaged Navier-Stokes (RANS) equations are widely used in the design and analysis of hypersonic airbreathing engine flow paths. These methods require models of statistical quantities of the turbulence in their development which have to be empirically calibrated and validated. In particular, new models for turbulent Schmidt and Prandtl number, as well as for turbulence-chemistry interactions, are required [1]. While suitable data is available for low-speed flows with combustion, sufficient data is still lacking in the area of supersonic combustion. Goyne et al. report measurements using particle-imaging velocimetry of mean streamwise velocity in a dual-mode scramjet [2]. At the NASA Langley Research Center, several data sets have been acquired in a  $H_2$  fueled supersonic combustor using the coherent anti-Stokes Raman spectroscopy (CARS) technique [3] and the dualpump CARS technique [4, 5]. The former technique gave temperature only while the latter gave both temperature and composition. Data included both mean flow and turbulent statistics, although the uncertainty in the latter was limited by both instrument precision and number of measurements from which the statistics were formed. International work in this area includes measurements in scramjet combustors conducted at ONERA (France) and DLR (Germany) using CARS [6], and other non-intrusive techniques.

Available data are limited to only a subset of the important variables (which are temperature, composition, density and velocity) in a limited number of geometries, and turbulence data are even rarer. To meet the need for more data, an Interferometric Rayleigh Scattering technique for measuring instantaneous velocity is being developed at the NASA Langley Research Center to complement the Dual-Pump CARS technique [7,8]. This technique uses Rayleigh scattering from one of the CARS laser beams to measure velocity in the same instant that CARS measures temperature and composition. Details on the techniques are given in a later section. Analysis of streams of such instantaneous measurements allows formation of the statistical quantities (means, variances, and covariances) required by modelers. Experimental configurations to provide suitable flow fields are being developed. An axisymetric coaxial free jet was selected since it provides the good optical access required for the Rayleigh technique, and symmetry can be taken advantage of to minimize the number of required spatial points. In order to form accurate statistics, large numbers of measurements are needed at each given point. The use of symmetry allows the total number of measurements to be made manageable. Another requirement of the flow field is that it should provide data that is relevant to both  $H_2$ - and hydrocarbon-fueled hypersonic air-breathing engines. The experiment should be capable of providing flows of various Mach numbers to establish the effects of compressibility. Finally, it is desirable to be able to create both supersonic combusting flows in which the flame is attached to the burner (flame held) and flows in which the flame is detached, since both types of flow can occur in hypersonic engine combustors. Figure 1 shows a schematic and photo of the coaxial free jet experiment. Figure 1(a) shows the burner and nozzle, sectioned along the axis, without bolts, tubes, spark plug and other fittings shown; Figure 1(b) is an image of the facility near the nozzle exit during operation, showing the supersonic jet of vitiated air and the laser beams of the CARS-Rayleigh system. The facility consists of a water-cooled combustion chamber (burner), a silicon carbide nozzle (sonic convergent, or supersonic convergent-divergent for M=1.6 and M=2), with an exit diameter of 10 mm and a coflow nozzle. Various combinations of gas flows to the burner are possible. In one set of experiments,  $H_2$  or  $CH_4$  fuel, air and  $O_2$ are reacted to provide vitiated air at various temperatures (dependent on flow rates). In these ex-

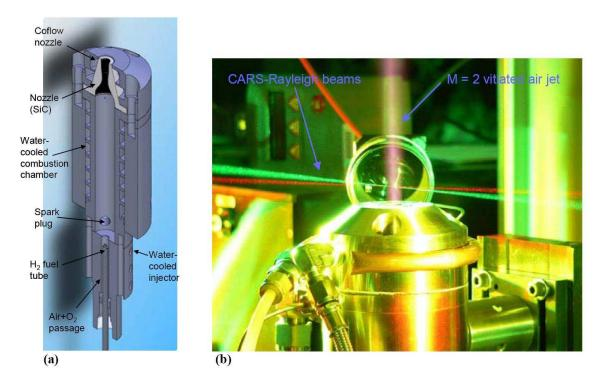


Figure 1: The supersonic jet combustor and nozzle. (a) Sectional view (without bolts, tubes, etc.). (b) Image during CARS-Rayleigh optical system data acquisition.

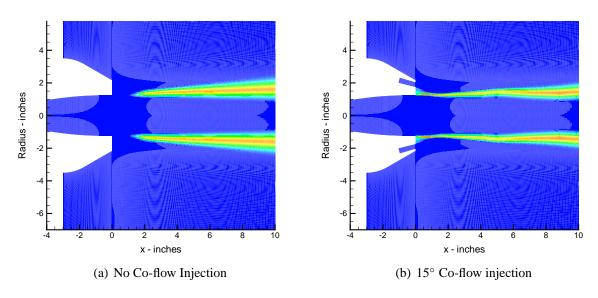


Figure 2: OH contours showing the sensitivity of the flame location to the presence of angled coflow injection.

Inner Jet				Outer Jet	
Mach No.	Heater Operation			Mach No.	Gas
1, 2	$H_2+O_2+$ Air vitiated	no unreacted $H_2$	one $T_{\circ}$	off	-
1, 2	$H_2+O_2+$ Air vitiated	$H_2$ rich	various $T_{\circ}$	off	-
1, 2	$H_2+O_2+Air$ vitiated	$H_2$ rich	various $T_{\circ}$	≤1	Air
1, 2	$H_2+O_2+$ Air vitiated	$O_2$ rich	various $T_{\circ}$	≤1	$CH_4$
1, 2	$CH_4+O_2+$ Air vitiated	$O_2$ rich	various $T_{\circ}$	≤1	$CH_4$
1, 2	$H_2+O_2+Air$ vitiated	$O_2$ rich	various $T_{\circ}$	≤1	$H_2$
1, 2	$CH_4+O_2+Air$ vitiated	$O_2$ rich	various $T_{\circ}$	≤1	$H_2$

Table 1: The experimental test matrix

periments, the coflow is of unheated  $H_2$  or  $CH_4$ , and the result (depending on temperature) is a mixing and reacting coaxial jet flow. In another set of experiments, the gas flows to the burner are  $H_2$ ,  $O_2$  or  $N_2$ , and air in such a ratio that the products contain excess  $H_2$ . The coflow is of air and the result again is a mixing and reacting coaxial jet flow. Depending on temperature and on the co-flow rate, the flame may be held at the annular base region formed between the central and coflow nozzle exits where the flow recirculates. Non-reacting cases can also be considered in the case where there is no excess  $H_2$  in the center jet and no fuel in the co-flow.

As part of the design effort, a parametric study of the proposed geometry and run conditions was conducted using CFD to determine the sensitivity of important experimental quantities, e.g. temperature, species, density and velocity, to a number of variables including: inner jet temperature, flame holding base size, co-axial jet injection angle, inner jet Mach number and sensitivity to computational values of the turbulent Prandtl and Schmidt numbers. An example calculation using the Vulcan CFD code [10] is shown in Figure 2, which shows the sensitivity of the flame location to the presence of a co-flow. This flow is with a Mach 2, hot hydrogen-rich inner jet without and with cold air co-flow.

Once the experimental geometry was finalized, CFD was used to help define the experimental test matrix. This matrix, given in Table 1, includes variations in the inner jet Mach number, the temperature of the inner jet, the type of fuel (hydrogen or methane), the equivalence ratio of the fuel and air and the location of the fuel and air streams (inner jet or co-flow jet). The CFD calculations completed in this step provide a baseline to compare with improved models planned for development using data from this and other experiments in the program. Figure 3 contains tables and flow images showing the various types of flames that are observed in the actual experiment. Two types of images are shown: visible light (true color images) with a long exposure time, and false color infrared (IR) images acquired in the 8 - 9 micron (long wave) region at an exposure time of 10 ms. The tables contain information pertaining to the state of the flame: no flame, detached flame, flame held at the base or at the external coflow boundary, and if the flame holding is marginal, i.e., at the point of extinction. Figure 3(a) pertains to cases with  $H_2$ -vitiated air in the center jet and  $H_2$  in the coflow. The center jet sensible enthalpy is varied by adjusting the flow rates from that of Mach 5.5 flight to that of Mach 7, and the exit Mach number of the center jet is either 1.0 or 2.0. The coflow is subsonic at the nozzle exit and the equivalence ratio (the ratio of  $H_2$  coflow rate to that required to consume all the  $O_2$  in the center jet,  $\phi$ ) is either 0.5 or 1. (It is not implied that the

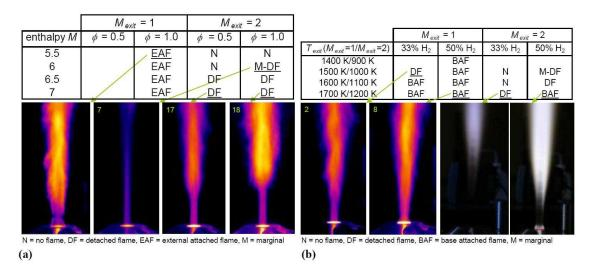


Figure 3: Flame state for a matrix of supersonic operating conditions at sonic and Mach 2 pressure matched exit conditions. Mixed infrared (false color) and visible light images (two right-most images). (a) Vitiated air center jet with subsonic hydrogen air coflow at an overall equivalence ratio  $\phi$ . (b) Hydrogen rich center jet with sonic coflow of air.

coflow  $H_2$  reacts only with the  $O_2$  in the center jet.) For  $M_{exit}=1$ , the flame is held at the exterior boundary in all cases, whereas, for  $M_{exit}=2$ , in some cases there is no flame and in others the flame is detached (stands off from the nozzle exit), but there are no cases with flame holding. With a detached flame, the trend with increasing center jet enthalpy is for the flame to move towards the nozzle exit. Figure 3(b) pertains to cases with excess  $H_2$  in the center jet, either 33% or 50% by volume of the jet flow being  $H_2$ . The exit static temperature is increased in increments of 100 K, and the exit Mach number is either 1.0 or 2.0. The coflow of air is sonic and pressure matched at the exit. In some cases, no flame is observed; in others, detached flames or flames attached at the base. The trend with increasing  $T_{exit}$  and decreasing  $M_{exit}$  is from no flame to detached flame to base-attached flame. Thus, a full range of flame behavior is attained which is ideal for model development and code validation.

Work has just begun to simulate the axisymmetric coaxial free jet experiment utilizing both RANS and LES codes. This work has not yet been completed. Work has been completed, however, on a coaxial jet mixing experiment that preceded the current work, and this experiment has been simulated using RANS codes. Details of the experiment are described in two earlier papers [11,12]. Low-density helium, which serves as a simulant of hydrogen fuel, was chosen to allow detailed studies of mixing without chemical reaction. Oxygen is added to the helium jet as a diagnostic aid for an oxygen flow-tagging technique (RELIEF). Several methods are utilized to characterize the flow field including Schlieren visualization, pitot pressure, total temperature, and gas sampling probe surveying, and RELIEF velocimetry. A schematic of the coaxial jet configuration is shown in Figure 4. The rig consists of a 10 mm inner nozzle from which helium, mixed with 5 percent oxygen by volume, is injected at Mach 1.8 and an outer nozzle 60 mm in diameter from which coflowing air is introduced also at Mach 1.8. The velocity ratio between the two jets is 2.25, the convective Mach number is 0.7, and the jet exit pressures are matched to one atmosphere. The

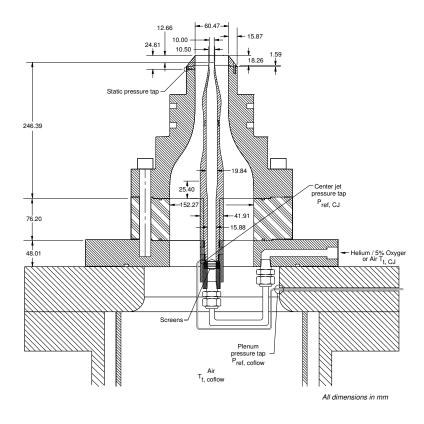


Figure 4: Coaxial jet assembly cross-section

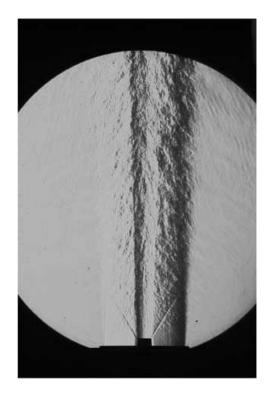


Figure 5: Schlieren image of coaxial jet mixing (conical extension cap removed)

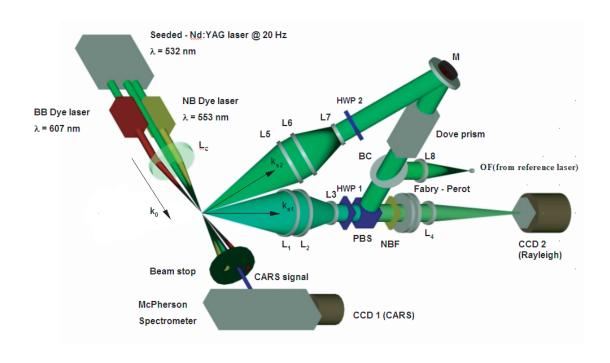


Figure 6: Experimental setup of the combined CARS - IRS system

resulting flow downstream of the nozzles can be seen in Figure 5, which shows a Schlieren image of the flowfield. The development of the mixing layer between the central helium jet and the air jet can be seen along with the shear layer development between the air jet and the surrounding quiescent laboratory air into which the air jet exhausts. Shock-expansion wave structure emanating outward from the centerbody nozzle lip can also be seen. Inward propagating waves from the inner lip, due to the finite thickness of the lip (0.25 mm), can be observed in the air jet once they pass through the helium jet. These waves are not visible in the helium jet due to the low refractive index within the center jet. A third wave can also be observed emanating inward from the outer nozzle lip and traversing both the air jet and the helium jet. The detailed data taken from this experiment along with the imaged shock-expansion structure provide an excellent case for assessing the ability of a reacting flow code to simulate complex mixing processes in a high-speed flow.

#### 3 Simultaneous CARS and Interferometric Rayleigh Scattering

It was recently reported [13] and is summarized here, the combination of a dual-pump coherent anti-Stokes Raman scattering system with an interferometric Rayleigh scattering system (CARS-IRS) to provide time-resolved simultaneous measurement of multiple properties in combustion flows. Time-resolved simultaneous measurement of temperature, absolute mole fractions of  $N_2$ ,  $O_2$ , and  $H_2$ , and two components of velocity in a Hencken burner flame were performed to demonstrate the technique. The experimental arrangement of the combined system is shown in Fig. 6. For the measurement of temperature and the absolute mole fractions of  $N_2$ ,  $O_2$ , and  $H_2$  a dual-pump

CARS method [4] is used. The system uses spectrally-narrow green (injection seeded Nd:YAG at 532 nm) and yellow (NB Dye laser at 552.9 nm) laser pump beams and one spectrally broad red laser (BB Dye laser at 607 nm) beam as the Stokes beam.

The beams are combined at the focusing point of a spherical lens Lc (focal length of 410 mm) in a folded BOXCARS geometry to probe Raman transitions of  $N_2$ ,  $O_2$  and  $H_2$ . The input beams plus the coherent blue signal beam at 491 nm are collected and collimated by another spherical lens with the same focal length as Lc. The three input beams are captured in a beam dump while the blue signal beam is passed to a spectrometer. The CARS signal, which is a spectrally broad blue beam that contains  $N_2$ ,  $O_2$  and  $H_2$  spectra, is analyzed by a spectrometer and recorded by the CCD1 camera. The shape of these spectra provides information on the temperature while the relative intensities of these spectra provide a measure of the relative mole fractions. The spectrum is fit with a theoretical model to determine the temperature and mole fractions.

The velocity measurement is performed simultaneously using an interferometric Rayleigh scattering measurement system [7]. The same pulsed, seeded green laser beam employed in the CARS technique is used as a narrow-band light source for the Rayleigh scattering system. The receiving optics for Rayleigh scattering are designed to capture the Rayleigh scattered light from the green pump beam in the measurement volume while preserving the scattering angle information, and to mix it together with the unshifted light of the laser before it is passed through the interferometer. In this way more than one component of velocity at multiple points can be measured in one interferogram [7, 14]. The velocity components measured are those that bisect the angles of laser's incidence and the collection optics. Since two directions are collected, two velocity components are measured. The Rayleigh scattered light from the two measurement directions are combined with a polarizing beam splitter (PBS) and directed through a Fabry-Perot etalon and onto a CCD camera for analysis (CCD2). The particular setup used here gives a range of measurable velocities from 0 to ~3 km/sec up to temperatures of about 2500 K. The CARS spectra and the Rayleigh spectra are acquired simultaneously by synchronizing the cameras with the green laser Q-switch pulse at 20 Hz. The spectra are subsequently processed, as described in reference [13] to determine the temperature, composition and velocity. To demonstrate the method, experiments were carried out in a Hencken burner, which provides an adiabatic  $H_2$ -air atmospheric pressure flame. The flame was stabilized with a co-flow of  $N_2$ . This flame was used because it provided a challenging high-temperature measurement environment while producing a known (near-zero) velocity.

Simultaneous CARS and Rayleigh scattering spectra up to 1610 K are shown in Fig. 7 (a-c) and in Fig. 7 (d-f), respectively: (a) and (d) are in the co-flow of  $N_2$ , (b) and (e) are in a high temperature flow containing  $N_2$  and  $O_2$ , and (c) and (f) are in a high temperature flow containing  $N_2$  and a low proportion of  $O_2$ . The CARS spectral plots show the experimental data, the theoretical fits, and also the residual between them. These spectra were used to calculate the rotational-vibrational gas temperature and the mole fraction of  $H_2$ ,  $O_2$ , and  $N_2$ .

For the Fabry-Perot spectra shown in Fig. 7, only one fringe order from each spectrum has been analyzed for this paper. The narrow shaped peak, more visible in the spectra of higher temperature, is the reference laser frequency (no Doppler shift). The broader spectrum is the Rayleigh scattered light. Each figure contains two Rayleigh and two reference spectra corresponding to the two collecting directions V1 (black trace) and V2 (red trace of smaller amplitude), differing by 34 degrees. Two-component velocity measurements in the range of 300-1600 K showed near-zero velocities

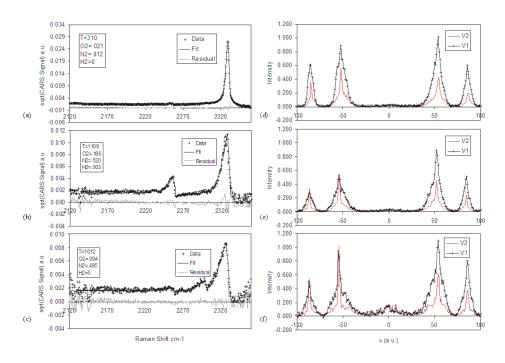
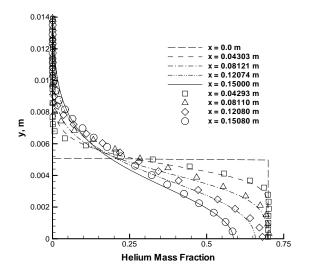


Figure 7: Simultaneous spectra of CARS (left) and Rayleigh scattering from two viewing directions (right). The CARS spectra are both data and fits of theory to the data. The Rayleigh spectra are data points connected by lines

(< 30 m/s) and standard deviations of 30-40 m/s. These errors are about 1% of the dynamic range of this measurement system (3,000 m/s). Measurement of one velocity component was shown to be possible at up to  $\sim$ 2,400 K with this system. These accuracies and precisions are within the desired range required for the planned supersonic combustion experiments where velocities will be up to 1,500 m/s. However, it is anticipated that future improvements in both hardware and software will allow these errors to be reduced by a factor of two or more.

#### 4 Simulation of Mixing and Reacting Flows

Improved numerical simulation of high-speed propulsion systems and engine performance relies on the development of enhanced codes with an increased capability to model turbulence, turbulent mixing, and kinetics. A significant amount of the design effort utilizes Reynolds averaged Navier-Stokes (RANS) codes for flowpath prediction. RANS design codes utilize phenomenological models to describe the turbulence field, fuel-air mixing, kinetics, and the interaction of turbulence and kinetics. There is an increased reliance on the use of large eddy simulation (LES) for the simulation of high-speed reacting flows [16]. LES methods calculate the large scale features of the flowfield and require modeling only to describe the small scale features of the flow utilizing a subgrid scale model. Subgrid scale models using filtered density functions (FDF) have shown great promise in improving the state-of-the-art in combustor modeling [17]. The FDF method is the counterpart of the probability density function (PDF) methodology, which has been long-established in RANS calculations of turbulent combustion [18]. The axisymmetric version of the SPARK RANS code



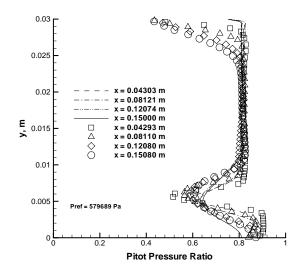


Figure 8: Comparison of helium mass fraction data (symbols) with simulation results

Figure 9: Comparison of pitot pressure data with simulation results

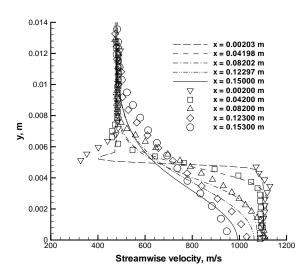


Figure 10: Comparison of RELIEF velocity data with simulation results

was used to simulate the flowfield in the helium/oxygen center nozzle and the outer air nozzle of the coaxial jet mixing experiment described in the previous experiment. Details of the code are given in reference [19]. The analysis of the experiment was begun by first solving for the flowfield in the center and outer nozzles. Results obtained at the end of each nozzle were then used to specify the supersonic inflow conditions for the downstream domain beyond the nozzles where mixing of the jets occurred. Details regarding the nozzle calculations and the mixing region downstream of the nozzles are given in reference [20].

A comparison of the measured helium mass fraction data with the simulation results at several stations downstream of the nozzles is given in Figure 8. Agreement between the simulation and the data is very good at each station. The code somewhat overpredicts the mixing near the centerline at the x = 0.12 m station, although the prediction improves with increasing radial distance. A comparison of measured pitot pressures with the simulation is shown in Figure 9. Agreement is good in the region of the air coflowing jet, but the simulation somewhat overpredicts the pitot pressure in the helium-air mixing region. The comparison with the experimental data differs at large radial distances greater than 0.025 m as the code does not consider the effects of the laboratory air entrained by the coaxial air jet. The RELIEF streamwise velocity data is compared with the simulation in Figure 10. The prediction agrees well with the data at the first three stations and slightly overpredicts the data at the remaining stations near the centerline. The simulation somewhat underpredicts the the velocity at the final three stations in the mixing region between the helium and air coflowing jets in agreement with the pitot pressure results.

## 5 Concluding Remarks

This paper has described work to develop phenomenological models for Reynolds averaged Navier-Stokes codes, subgrid scale models for use in large-eddy simulation and reduced-kinetics mechanisms to model hydrogen-air and hydrocarbon-air reaction in propulsion applications. Fundamental experiments are being performed to provide data that will be used in the development and refinement of these models. Experimental data is extracted from the experiments using nonintrusive diagnostics that allow accurate simultaneous measurement of temperature, species, and up to three components of velocity in supersonic flow without changing the character of the flowfield. Once the databases are in hand, the data will be analyzed using a response surface methodology [21–23] that provides an efficient means of determining critical parameters in a chosen model. The models will then be incorporated into combustion codes used in engine flowpath analysis and design.

#### References

- [1] Baurle, R.A., "Modeling of High Speed Reacting Flows: Established Practices and Future Challenges," AIAA 2004-267, 42nd Aerospace Sciences Meeting and Exhibit, Reno, NV, 5-8 Jan, 2004.
- [2] Goyne, C.P., McDaniel, J.C., Krauss, R.H., Day, S.W., "Velocity measurement in a dual-mode supersonic combustor using particle image velocimetry," AIAA Paper 2001-1761, AIAA/NAL-NASDA-ISAS International Space Planes and Hypersonic Systems and Technologies Conference, 10th, Kyoto, Japan, Apr. 24-27, 2001.
- [3] Cutler, A.D., Danehy, P.M., Springer, R.R., O'Byrne, S., Capriotti, D.P., DeLoach, R., "Coherent Anti-Stokes Raman Spectroscopic Thermometry in a Supersonic Combustor," AIAA J., Vol. 41, No. 12, Dec. 2003.

- [4] O'Byrne, S., Danehy, P.M., Cutler, A.D., "Dual-Pump CARS Thermometry and Species Concentration Measurements in a Supersonic Combustor," AIAA Paper 2004-0710, 42nd Aerospace Sciences Meeting, Reno, NV, Jan. 5-8, 2004.
- [5] Tedder, S. A., O'Byrne, S., Danehy, P. M., Cutler, A. D., "CARS Temperature and Species Concentration Measurements in a Supersonic Combustor with Normal Injection," AIAA Paper 2005-0616, 43rd AIAA Aerospace Sciences Meeting, Reno, NV, Jan 10-13, 2005.
- [6] Bresson, A., Bouchardy, P., Magre, P., Grisch, F., "OH/acetone PLIF and CARS thermometry in a supersonic reactive layer," AIAA Paper 2001-1759, AIAA/NAL-NASDA-ISAS International Space Planes and Hypersonic Systems and Technologies Conference, 10th, Kyoto, Japan, Apr. 24-27, 2001.
- [7] Bivolaru, D., Danehy, P.M., Lee, J.W., Gaffney, R.L., Cutler, A.D., "Single-pulse, Multi-point Multi-component Interferometric Rayleigh Scattering Velocimeter," AIAA-2006-0836, 44th AIAA Aerospace Sciences Meeting, Reno, NV, 9-12 Jan., 2006.
- [8] Bivolaru, D., Otugen, M. V., Tzes, A. and Papadopoulos, G., "Image Processing for Interferometric Mie and Rayleigh Scattering Velocity Measurements," AIAA Journal, Vol. 37, No. 6, pp. 688-694, 1999.
- [9] Gaffney, Richard L. Jr., Cutler, Andrew D., "CFD Modeling Needs And What Makes A Good Supersonic Combustion Validation Experiment," JANNAF CS/APS/PSHS/MSS Joint Meeting, Charleston, SC, June, 2005.
- [10] White, J. A. and Morrison, J. H., "A Pseudo-Temporal Multi-Grid Relaxation Scheme for Solving the Parabolized Navier-Stokes Equations," AIAA paper no. 99-3360, June, 1999.
- [11] Cutler, A. D., Carty, A., Doerner, S., Diskin, G., and Drummond, J. P., Supersonic Coaxial Jet Flow Experiment for CFD Code Validation. AIAA Paper 99-3588, June 1999.
- [12] Cutler, A. D., and White, J. A., An Experimental and CFD Study of a Supersonic Coaxial Jet. AIAA Paper 2001-0143, January 2001.
- [13] D. Bivolaru, P. M. Danehy, K. D. Grinstead, Jr., S. Tedder, A. D. Cutler, "Simultaneous CARS and Interferometric Rayleigh Scattering," AIAA AMT-GT Technology Conference, San Francisco, AIAA-2006-2968 June (2006).
- [14] Bivolaru, D., Danehy, P. M., and Lee, J. W, "Intracavity Rayleigh-Mie Scattering for multipoint, two-component velocity measurement," Optics Letters, Vol. 31, No. 11, pp. 1645-1647, June, 2006.
- [15] Cutler, A. D., Danehy, P. M., Byrne, P.O., Rodriguez, C.G., and Drummond, J. P., "Supersonic Combustion Experiments for CFD Model Development and Validation," AIAA 2004-0266, 2004.
- [16] Janicka, J. and Sadiki, A., Large eddy simulation of turbulent combustion systems. *Proc. Combust. Inst.* **30** (2005) 537–547.
- [17] Givi, P., Filtered density function for subgrid scale modeling of turbulent combustion. *AIAA J.* **44**(1) (2006) 16–23.
- [18] Pope, S. B., Turbulent Flows. Cambridge, UK: Cambridge University Press (2000).
- [19] Drummond, J. P., Numerical Simulation of a Supersonic Chemically Reacting Mixing Layer. NASA TM 4055, 1988.
- [20] Drummond, J. P., Diskin, G. S. and Cutler, A. D., Fuel-Air Mixing and Combustion in Scramjets. AIAA Paper 02-3878, July 2002.
- [21] Box, G.E.P. and Wilson, K.B., "On the Experimental Attainment of Optimum Conditions," *Journal of the Royal Statistical Society* Ser.B, 13, pp. 195–241, 1951.
- [22] Montgomery, D. C., Design and Analysis of Experiments, 6th edition, John Wiley & Sons, 2004.
- [23] Myers, R. H. and Montgomery, D. C., Response Surface Methodology: Process and Product Optimization Using Designed Experiments, 2nd edition, John Wiley & Sons, 2002.